



ORIGINAL ARTICLE

Metabolism studies of 4'Cl-CUMYL-PINACA, 4'F-CUMYL-5F-PINACA and 4'F-CUMYL-5F-PICA using human hepatocytes and LC-QTOF-MS analysis

Darta Stalberga¹  | Sarah Ingvarsson^{2,3} | Ghidaa Bessa³ | Lisa Maas^{2,4} | Svante Vikingsson^{1,2,5} | Mattias Persson² | Caitlyn Norman⁶  | Henrik Gréen^{1,2}

¹Division of Clinical Chemistry and Pharmacology, Department of Biomedical and Clinical Sciences, Faculty of Medicine, Linköping University, Linköping, Sweden

²Department of Forensic Genetics and Forensic Toxicology, National Board of Forensic Medicine, Linköping, Sweden

³Department of Physics, Chemistry and Biology, Linköping University, Linköping, Sweden

⁴Avans University of Applied Sciences, Breda, Netherlands

⁵Center for Forensic Sciences, RTI International, Research Triangle Park, North Carolina, USA

⁶Leverhulme Research Centre for Forensic Science, School of Science and Engineering, University of Dundee, Dundee, UK

Correspondence

Division of Clinical Chemistry and Pharmacology, Department of Biomedical and Clinical Sciences, Faculty of Medicine, Linköping University, Linköping SE-581 85, Sweden.
Email: stalberga.darta@gmail.com

Funding information

VINNOVA, Grant/Award Number: 2019-03566; Eurostars-2 Joint Programme, Grant/Award Number: E! 113377, NPS-REFORM; European Union's Horizon 2020; Sweden's Innovation Agency Vinnova; Strategic Research Area in Forensic Sciences, Grant/Award Number: 2016:7

Abstract

4'Cl-cumyl-PINACA (SGT-157), 4'F-cumyl-5F-PINACA (4F-cumyl-5F-PINACA, SGT-65) and 4'F-cumyl-5F-PICA (4F-cumyl-5F-PICA, SGT-64) are a series of new halogenated cumyl synthetic cannabinoid receptor agonists (SCRAs). Due to rapid metabolism, monitoring and screening for SCRAs in biological matrices requires identification of their metabolites. It is an essential tool for estimating their spread and fluctuations in the global illicit market. The purpose of this study was to identify human biotransformations of 4'Cl-cumyl-PINACA, 4'F-cumyl-5F-PINACA and 4'F-cumyl-5F-PICA in vitro and characterize for the first time the metabolic pathways of halogenated cumyl SCRAs. 4'Cl-cumyl-PINACA, 4'F-cumyl-5F-PINACA and 4'F-cumyl-5F-PICA were incubated with human hepatocytes in duplicates for 0, 1, 3 and 5 h. The supernatants were analysed in data-dependent acquisition on a UHPLC-QToF-MS, and the potential metabolites were tentatively identified. A total of 11 metabolites were detected for 4'Cl-cumyl-PINACA, 21 for 4'F-cumyl-5F-PINACA and 10 for 4'F-cumyl-5F-PICA. The main biotransformations were oxidative defluorination, followed by hydroxylation with dehydrogenation, N-dealkylation, dihydrodiol formation and glucuronidation. Hydroxylations were most common at the tail moieties with higher abundance for indole than indazole compounds. N-dealkylations were more common for fluorinated tail

Sarah Ingvarsson, Ghidaa Bessa and Lisa Maas contributed equally.

This is an open access article under the terms of the [Creative Commons Attribution-NonCommercial](https://creativecommons.org/licenses/by-nc/4.0/) License, which permits use, distribution and reproduction in any medium, provided the original work is properly cited and is not used for commercial purposes.

© 2022 The Authors. *Basic & Clinical Pharmacology & Toxicology* published by John Wiley & Sons Ltd on behalf of Nordic Association for the Publication of BCPT (former Nordic Pharmacological Society).

chain compounds than the non-fluorinated 4'-Cl-cumyl-PINACA. In conclusion, many metabolites retained halogen groups at the cumyl moieties which, in various combinations, may be suitable as analytical biomarkers.

KEYWORDS

human hepatocytes, metabolism, metabolites, new psychoactive substances, synthetic cannabinoids

1 | INTRODUCTION

New psychoactive substances (NPSs), commonly known as legal highs, designer drugs and research chemicals, have become a widespread and persistent problem for public health and society. These substances have psychoactive effects resembling those of traditional drugs of abuse, and their chemical structures are constantly changed by clandestine laboratories in order to circumvent new or revised national and international legislation.¹

Synthetic cannabinoid receptor agonists (SCRAs) represent the largest group of NPS that are currently monitored in Europe by the European Monitoring Centre for Drugs and Drug Addiction (EMCDDA) through the EU Early Warning System. By the end of December 2021, the EMCDDA was monitoring 224 SCRAs that had appeared on the drug market since 2008. Between 2011 and 2015, during the peak of the “legal highs” phenomenon, an average of 27 SCRAs appeared on the drug market in Europe each year. Since 2016, the number dropped to around 10 annually with a slight increase to 15 new SCRAs in 2021.¹

SCRAs are substances that activate the cannabinoid receptors, CB₁ and CB₂.^{2,3} These compounds cause a range of neurological and physiological effects mainly mediated by activation of the CB₁ receptor.^{4–7} SCRAs have been associated with both fatal and non-fatal poisonings/intoxications worldwide⁸ and are particularly prevalent in vulnerable groups such as rough sleeping populations (anyone who is living on the streets, sleeping in parks or squatting in derelict buildings for temporary shelter) and prisoners.¹ Therefore, it is important to monitor these compounds in forensic samples, which is complicated by the constant structural evolution of NPSs.

SCRAs are a structurally diverse group of NPSs with an elaborate universal characterization scheme. Their structures are subdivided into four constituent moieties—head, linker, core and tail (see Figure 1). The addition of a halogen atom, most often fluorine, on the tail moiety is a common structural change made by clandestine producers.^{1,5,9} From a pharmacological point of view, adding halogens often changes the polarity and electronegative charge of a molecule. This can drastically change both the activity and the metabolism of the

compounds.¹⁰ It has been shown that terminal fluorination of the tail moiety of N-pentyl indole SCRAs in most cases increases the potency at the CB₁ receptor.⁵ Similar potency increases due to terminal fluorination of the tail moiety have also been detected for SCRAs with a cumyl head moiety, for example, cumyl-PICA (EC₅₀ 4.2 and 11.98 nM) to cumyl-5F-PICA (EC₅₀ 2.8 and 5.83 nM) and cumyl-PINACA (EC₅₀ 2.3 nM) to cumyl-5F-PINACA (EC₅₀ 0.43 nM).^{9,11} Although Asada et al. reported a similar increase in potency for cumyl-5F-PICA (from 777 to 20.9 nM), they observed a decrease in potency from cumyl-PINACA (EC₅₀ 5.12 nM) to cumyl-5F-PINACA (EC₅₀ 15.1 nM).¹² Similarly, Gamage et al. reported a small decrease in 5F-cumyl-PICA potency (from 1.33 to 2.34 nM) by an alternative pathway activation.¹¹ The difference could be due to the different evaluation methods used by the research groups.^{9,11,12}

The cumyl head moiety has become more frequent among SCRAs on the illicit market (e.g., cumyl-PINACA, cumyl-4CN-BINACA and cumyl-FUBICA) since its invention and publication in a patent from Stargate International (New Zealand) in 2014.¹³ Included in this patent were SGT-157 (4'-Cl-cumyl-PINACA), SGT-65 (4F-cumyl-5F-PINACA also known as 4'-F-cumyl-5F-PINACA) and SGT-64 (4F-cumyl-5F-PICA also known as 4'-F-cumyl-5F-PICA). While casework detections of these compounds have not been reported, they have been mentioned on psychonaut/user forums, indicating some use of these compounds in the community.¹⁴ These compounds are available as reference standards from different vendors and mass spectra are available as a result of project RESPONSE.¹⁵ However, despite the present structural knowledge about these SCRAs with direct halogenation of the cumyl moiety, the metabolic and pharmacological characterization is still missing.

Metabolite characterization is an important task for drug monitoring since many SCRAs are rapidly metabolized making the detection of the parent compound challenging.^{16,17} Furthermore, the variable lipophilic nature of SCRAs and their wide distribution in adipose tissues and the cardiovascular system further impacts their detection limits.^{18,19} In acute cases, the parent compound can be detected in serum for up to 20 h; however, the most common matrix used for the

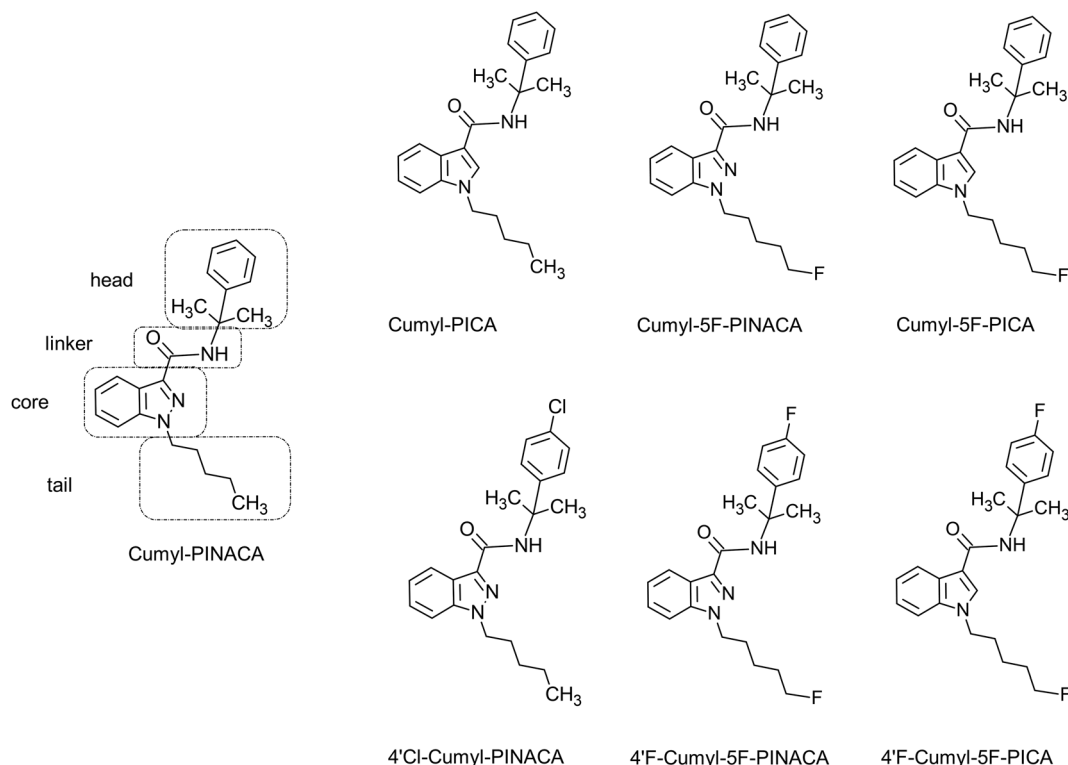


FIGURE 1 Structures of cumyl-PINACA, cumyl-PICA, cumyl-5F-PINACA, cumyl-5F-PICA and the analogue SCRA used in this study 4'Cl-cumyl-PINACA, 4'F-cumyl-5F-PINACA and 4'F-cumyl-5F-PICA.

detection of drugs in urine, mostly due to non-invasive sampling.^{16,17,19} Identification of metabolites and their characterization is therefore important as a basis for expanding screening to a variety of structurally related compounds. For structurally related compounds that share the same metabolites, usually more than one characteristic metabolite is assigned as the biomarker of each compound.^{16,20,21}

This study aimed to characterize the metabolism of three novel SCRA: 4'Cl-cumyl-PINACA, 4'F-cumyl-5F-PINACA and 4'F-cumyl-5F-PICA. The metabolites were identified with ultra-high performance liquid chromatography coupled with a quadrupole time of flight mass spectrometer (UHPLC-QToF-MS) following incubation of the SCRA with pooled human hepatocytes. The acquired data were used to identify potential metabolites, propose a metabolic pathway for each substance and suggest feasible biomarkers for forensic diagnostics. The pathways were also compared with those of related substances to find common structure-related patterns.

2 | METHODS

In this study, the SCRA 4'Cl-cumyl-PINACA, 4'F-cumyl-5F-PINACA and 4'F-cumyl-5F-PICA were incubated with pooled cryopreserved human hepatocytes in duplicates

for 0–5 h. Formed metabolites were analysed with LC-QToF-MS and identified by their MS/MS spectra using Mass Hunter Qualitative Analysis B.07.00 software.

2.1 | Chemicals and reagents

All cryopreserved hepatocytes and inVitro Gro HT thawing medium were obtained from Bioreclamation IVT (Brussels, Belgium). LiverPool 10 donor pool hepatocytes were used for incubations with 4'Cl-cumyl-PINACA and 4'F-cumyl-5F-PINACA while 20 donor pool hepatocytes were used with 4'F-cumyl-5F-PICA.

LC-MS grade methanol was purchased from Merck (Darmstadt, Germany). HPLC grade acetonitrile (ACN); LC/MS grade formic acid; Williams E medium; L-glutamine; HEPES buffer; trypan blue 0.4% solution; the internal standard solution mixture of D₈-amphetamine 15 µg/ml, D₅-diazepam 5 µg/ml, D₃-mianserin 2.5 µg/ml and D₅-phenobarbital 15 µg/ml; and the positive control stock of caffeine 5 mg/ml, bupropion 1 mg/ml, diclofenac 1 mg/ml, omeprazole 1 mg/ml, dextromethorphan 1 mg/ml, chlorzoxazone 1 mg/ml and midazolam 1 mg/ml were obtained from Thermo Fisher Scientific (Gothenburg, Sweden).

4'Cl-cumyl-PINACA (purity ≥ 99.0%, IUPAC name: N-[2-(4-chlorophenyl)propan-2-yl]-1-pentyl-1H-indazole-

3-carboxamide), 4'-F-cumyl-5F-PINACA (purity $\geq 100\%$, IUPAC name: 1-(5-fluoropentyl)-N-[2-(4-fluorophenyl)propan-2-yl]-1H-indazole-3-carboxamide) and 4'-F-cumyl-5F-PICA (purity $\geq 98.8\%$, IUPAC name: 1-(5-fluoropentyl)-N-[2-(4-fluorophenyl)propan-2-yl]-1H-indole-3-carboxamide) were obtained from Cayman Chemicals (Ann Arbor, MI, USA) and diluted to 1 mg/ml in methanol.

2.2 | Incubation with hepatocytes and sample preparation

In this study, the three SCRA were incubated with pooled human hepatocytes for 0, 1, 3 and 5 h in duplicates.

The cryopreserved hepatocytes were thawed and transferred to 48-ml inVitro Gro HT media preheated to 37°C, centrifuged at room temperature (RT) for 5 min at 100g and washed twice with 50-ml Williams E medium supplemented with 2-mM L-glutamine and 20-mM HEPES buffer. Using the 0.4% trypan blue exclusion method, the cell concentration was adjusted to 2×10^6 cells/ml with supplemented Williams E medium.

The 1-mg/ml SCRA solutions were diluted to 10 μ M in supplemented Williams E medium. 50 μ l of this SCRA working solution and 50 μ l of the hepatocyte solution were mixed in 96-well plates. The hepatocytes were incubated for 0, 1, 3 and 5 h at 37°C, 5% CO₂ and the reactions were quenched by 100- μ l ice-cold ACN mixed with the internal standard solution (diluted in methanol with final concentrations of 150-ng/ml D₈-amphetamine, 50-ng/ml D₅-diazepam, 25-ng/ml D₃-mianserin and 150-ng/ml D₅-phenobarbital). For the 0 h, the ice-cold ACN mix was added to the wells before the hepatocytes. Positive control wells consisted of hepatocytes and the positive control stock (diluted in methanol with the final concentration of 500 μ M) containing compounds selectively metabolized by CYP 450 1A2, 2B6, 2C9, 2C19, 2D9, 2E1 and 3A4; the negative control wells consisted of hepatocytes and medium; and the degradation control wells contained SCRA solutions and medium. All control samples were incubated for 3 h. After terminating the reaction, the plates were shaken for 2 min at RT at 600 rpm, placed at -20°C for 10 min and centrifugated for 10–15 min at 1100g at 4°C. 120 μ l of the supernatants was transferred to an injection plate and used for the LC-QToF-MS experiments.

2.3 | LC-QToF-MS analysis

To identify the produced metabolites, 4 μ l of the supernatant was injected into the LC-QToF-MS system composed of an Agilent 1290 infinity Ultra-High-

Performance Liquid Chromatography (UHPLC) system (Agilent Technologies, Kista Sverige) coupled with an Agilent 6550 iFunnel QToF mass spectrometer (Agilent Technologies, Kista, Sweden) with a dual Agilent Jet Stream electrospray ionization source. UHPLC separation was achieved with an Acquity HSS T3 column (150 mm \times 2.1 mm, 1.8 μ m; Waters, Sollentuna, Sweden) fitted with an Acquity Van Guard pre column (Waters, Sollentuna, Sweden) kept at 60°C. The initial mobile phase composition was 99% mobile phase A, 0.1% formic acid in MilliQ water and 1% mobile phase B, 0.1% formic acid in ACN. The gradients were pre-selected to ensure retention of the parent compounds between 10 and 13 min, and the same gradient program was used for all three substances. The flow rate was 0.500 ml/min. The gradient was 1% B (0–0.6 min), 1%–20% B (0.6–0.7 min), 20%–85% B (0.7–13 min), 85%–95% B (13–15 min), 95% B (15–18 min), 95%–1% B (18–18.1 min) and 1% B (18.1–19 min).

The QToF-MS was operated in positive electrospray ionization mode. The used parameters were gas temperature, 150°C; gas flow, 18 L/min; nebulizer gas pressure, 345 kPa; sheath gas temperature, 375°C; and sheath gas flow, 11 L/min. For metabolite identification, Auto MS/MS acquisition mode was used with parameters: scan rate, 6 spectra/s (MS) and 10 spectra/s (MS/MS); scan range, 100–950 m/z; precursor intensity threshold, 5000 counts; precursor number per cycle, 5; precursor isolation width ~ 1.3 m/z; fragmentor voltage, 380 V; and collision energy (CE), 3 eV at 0 m/z ramped up by 8 eV per 100 m/z.

2.4 | Data analysis

A library of potential metabolites, including hydroxylations, dehydrogenations, oxidative and non-oxidative defluorinations/dechlorinations, N-dealkylations, dihydrodiol formation, glucuronidations and combinations thereof, was compiled. Using the library, metabolites were identified with the Agilent MassHunter Qualitative analysis (version B.07.00) software. The search was performed with the following parameters: mass error, 50 ppm; absolute peak area threshold, 20 000 counts; the maximum number of matches, 20; and extraction window, 100 ppm. The metabolites were identified if mass errors of protonated molecules were < 5 ppm (unless saturated peak), the retention time was between 4 and 15 min, an MS/MS spectra was present, peak area was > 20 000, peak absence in negative controls and degradation controls and an isotopic pattern were consistent with the parent compound and positive control compounds were metabolized accordingly to their selective enzymes. All the biotransformations and the potential structures of

the metabolites were identified based on the HRMS m/z and the MS/MS spectra. After metabolite identification in ≥ 1 sample, other incubation samples were manually assessed for the metabolite presence at lower abundance with peak area below the set threshold of 20 000. Further confirmation was based on the retrieved MS/MS fragmentation pattern.

The study was conducted in accordance with the Basic & Clinical Pharmacology & Toxicology policy for experimental and clinical studies.²²

3 | RESULTS

From incubations with human hepatocytes, in total 11 metabolites were identified for 4'-Cl-cumyl-PINACA, 21 metabolites for 4'-F-cumyl-5F-PINACA and 10 metabolites for 4'-F-cumyl-5F-PICA. The metabolites are numbered in this article according to their total peak area, from the highest to the lowest total area detected.

The most common biotransformations included hydroxylations, hydroxylations with dehydrogenation, N-dealkylations, oxidative defluorinations and glucuronidations in various combinations. The MS/MS spectra and the fragmentation patterns of the parent compounds are shown in Figure 2. The identified metabolites are listed in Tables 1, 2 and 3 with the diagnostic fragment ions, respective retention times, formulae, mass errors and peak areas obtained from 1-, 3- and 5-h incubations. Figures of the mass spectra and the proposed fragmentation patterns of all the metabolites can be found in the Supporting Information.

3.1 | The metabolic profile of 4'-Cl-cumyl-PINACA

All 11 metabolites (A1–A11) of 4'-Cl-cumyl-PINACA had a retention time between 7.03 and 11.12 min while the parent compound had the highest retention time

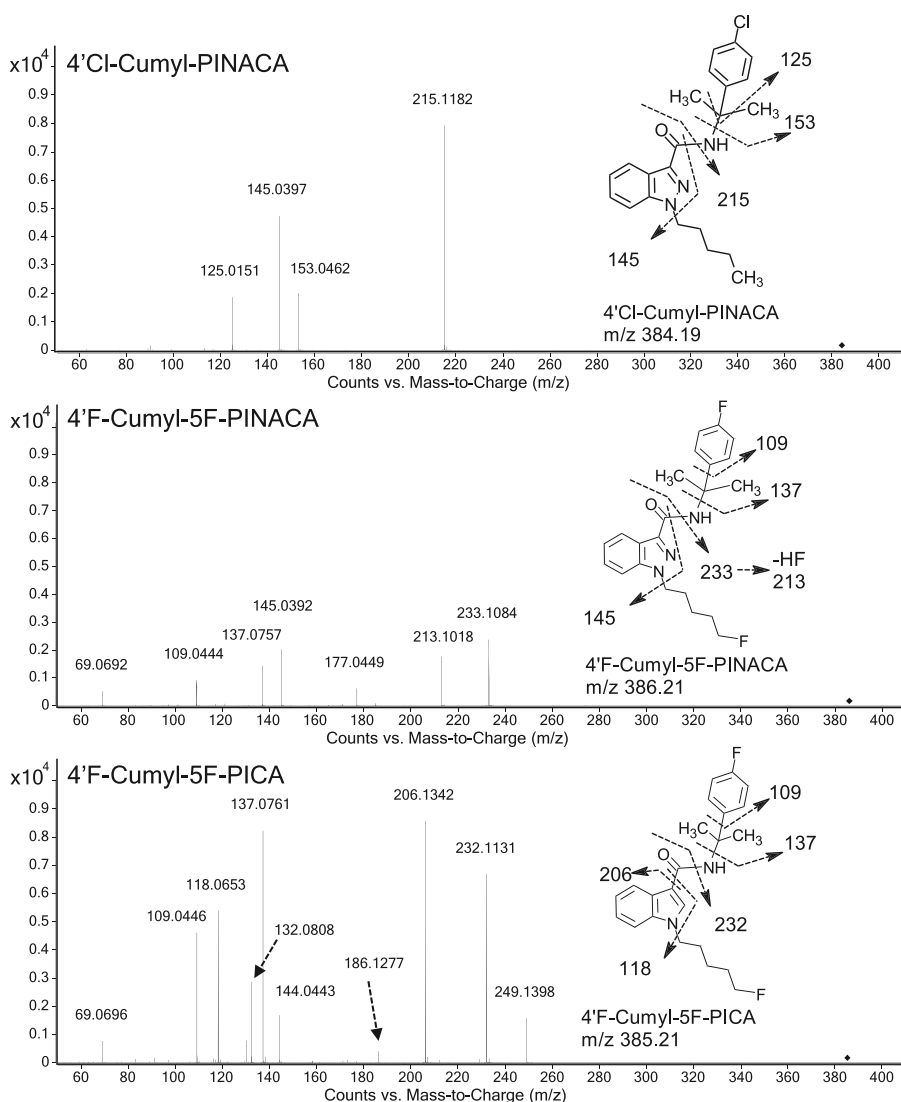


FIGURE 2 The MS² spectra and the fragmentation patterns of the parent compounds 4'-Cl-cumyl-PINACA, 4'-F-cumyl-5F-PINACA and 4'-F-cumyl-5F-PICA. Elaborated peak structures are presented in the Supporting Information.

T A B L E 1 4'Cl-Cumyl-PINACA metabolites with biotransformation, molecular formula, retention time, mass errors (minimum and maximum), exact mass (m/z) of protonated molecules and peak areas at 1-, 3- and 5-h incubation time

Met-ID	Compound name	Molecular formula	Retention time (min)	Obs m/z (M + H)	ppm min	ppm max	1 h #1 A/1000	1 h #2 A/1000	3 h #1 A/1000	3 h #2 A/1000	5 h #1 A/1000	5 h #2 A/1000	Grand total	Major fragment ions
A0	Parent	C22 H26 Cl N3 O	13.66	384.1854	0.56	4.66	6747	7258	10 703	12 030	13 758	13 569	64 065	125, 145, 153, 215
A1	MonoOH with dehydrogenation	C22 H24 Cl N3 O2	10.61	398.1630	-0.48	-1.9	1008	1101	694	784	511	488	4587	85, 125, 145, 153, 229
A2	MonoOH	C22 H26 Cl N3 O2	9.99	400.1786	-0.07	1.43	783	801	431	483	284	278	3060	125, 145, 153, 213, 231
A3	DiOH	C22 H26 Cl N3 O3	8.53	416.1732	-0.66	-2.5	348	348	309	325	265	250	1843	85, 125, 145, 153, 229, 247
A4	MonoOH	C22 H26 Cl N3 O2	10.54	400.1784	-0.56	-1.89	402	391	243	273	210	190	1708	125, 145, 153, 231
A5	DiOH with dehydrogenation	C22 H24 Cl N3 O3	9.37	414.1575	-1.49	-3.22	340	371	254	299	163	163	1590	55, 101, 125, 145, 153, 245
A6	DiOH	C22 H26 Cl N3 O3	8.38	416.1731	-0.49	5.27	220	218	236	252	198	181	1305	85, 125, 145, 153, 229, 247
A7	MonoOH with dehydrogenation	C22 H24 Cl N3 O2	11.12	398.1624	-1.35	-2.91	192	202	183	198	136	135	1046	57, 85, 125, 145, 153, 229
A8	MonoOH + GLUC	C28 H34 Cl N3 O8	7.82	576.2101	0.05	-3.4	62	62	274	177	220	214	1009	145, 153, 213, 231
A9	DiOH with dehydrogenation	C22 H24 Cl N3 O3	9.55	414.1573	-0.5	-2.34	88	80	257	191	180	174	970	125, 145, 153, 217, 227
A10	N-dealkylation	C17 H16 Cl N3 O	9.12	314.1050	0.24	-0.93	106	98	114	113	103	105	640	125, 145, 153
A11	TriOH	C22 H26 Cl N3 O4	7.03	432.1676	-1.69	-3.14	44	44	78	74	74	71	385	85, 125, 153, 263

Abbreviations: DiOH, dihydroxylation; GLUC, glucuronidation; MonoOH, monohydroxylation; TriOH, trihydroxylation.

T A B L E 2 4'-F-Cumyl]-5F-PINACA metabolites with biotransformation, molecular formula, retention time, mass errors (minimum and maximum), exact mass (m/z) of protonated molecules and peak areas at 1-, 3- and 5-h incubation time

Met-ID	Compound name	Molecular formula	Retention time (min)	Obs m/z (M + H)	ppm min	ppm max	1 h #1 A/1000	1 h #2 A/1000	3 h #1 A/1000	3 h #2 A/1000	5 h #1 A/1000	5 h #2 A/1000	Grand total	Major fragment ions
E0	Parent	C22 H25 F2 N3 O	11.43	386.2054	2.4	4.3	16 843	17 705	3966	6763	4198	6613	56 087	109, 137, 145, 213, 233
E1	Oxidative defluorination	C22 H26 F N3 O2	9.06	384.2088	-0.2	3.1	3320	3359	1259	1758	1718	1444	12 859	69, 109, 137, 145, 213, 231
E2	Oxidative defluorination and monoOH	C22 H26 F N3 O3	7.31	400.2033	-0.5	0.9	1758	1769	703	1248	1485	2092	9055	109, 137, 145, 175, 229, 247
E3	MonoOH	C22 H25 F2 N3 O2	8.96	402.1991	-0.1	1.6	3301	3424	411	770	385	552	8842	109, 137, 145, 231, 249
E4	N-dealkylation	C17 H16 F N3 O	8.19	298.1354	0.9	1.7	1583	1775	613	1009	1441	1801	8222	109, 137, 145
E5	MonoOH	C22 H25 F2 N3 O2	9.12	402.1991	-0.8	1.8	3139	3210	357	661	346	432	8145	85, 109, 137, 145, 249
E6	Oxidative defluorination +GLUC	C28 H34 F N3 O8	7.12	560.2407	-0.1	1.2	446	442	1067	1185	1284	1299	5724	109, 137, 145, 213, 231
E7	MonoOH with dehydrogenation	C22 H23 F2 N3 O2	9.70	400.1829	-1.8	0.3	934	1027	119	254	159	226	2718	109, 137, 145, 177, 227, 247
E8	MonoOH	C22 H25 F2 N3 O2	9.31	402.1985	-1.9	0.4	857	888	98	195	124	166	2328	109, 137, 145, 249
E9	Oxidative defluorination and dihydrodiol formation	C22 H28 F N3 O4	5.72	418.2133	-2.0	0.1	156	153	156	197	246	279	1186	69, 109, 137, 179, 247, 265
E10	Dihydrodiol	C22 H27 F2 N3 O3	7.64	420.2089	-2.1	-0.5	256	256	72	120	103	141	948	69, 109, 137, 179, 247, 267
E11	MonoOH +GLUC	C28 H33 F2 N3 O8	7.04	578.2298	-2.8	-1.2	104	100	151	176	160	170	861	109, 137, 145, 249

(Continues)

TABLE 2 (Continued)

Met-ID	Compound name	Molecular formula	Retention time (min)	Obs m/z (M + H)	ppm min	ppm max	1 h #1 A/1000	1 h #2 A/1000	3 h #1 A/1000	3 h #2 A/1000	5 h #1 A/1000	5 h #2 A/1000	Grand total	Major fragment ions
E12	Oxidative defluorination, monoOH with dehydrogenation	C22 H24 F N3 O3	7.92	398.1859	-5.6	-2.3	99	112	57	86	198	102	653	137, 145, 175, 227, 245
E13	Oxidative defluorination, monoOH with dehydrogenation	C22 H24 F N3 O3	8.15	398.1865	-3.2	-1.8	155	171	48	76	0	173	622	101, 109, 137, 145, 227, 245
E14	Oxidative defluorination and diOH	C22 H26 F N3 O4	5.84	416.1973	-3.6	-1.4	108	120	59	74	101	109	572	145, 231, 249
E15	MonoOH + GLUC	C28 H33 F2 N3 O8	6.91	578.2302	-1.8	-0.8	69	64	103	112	101	92	541	109, 137, 145, 231, 249
E16	Dihydrodiol and monoOH	C22 H27 F2 N3 O4	5.71	436.2035	-2.4	-1.1	81	82	58	76	95	96	489	109, 137, 161, 179, 265, 283
E17	N-dealkylation and monoOH	C17 H16 F N3 O2	6.70	314.1290	-3.8	-1.4	34	38	44	59	152	150	478	109, 137, 161
E18	Oxidative defluorination and diOH	C22 H26 F N3 O4	6.03	416.1971	-5.3	-0.3	92	104	38	54	69	72	429	67, 108, 117, 145, 177, 249
E19	Dihydrodiol and monoOH	C22 H27 F2 N3 O4	6.09	436.2035	-4.4	-0.8	74	74	44	63	76	83	414	67, 109, 137, 161, 193, 283
E20	DiOH	C22 H25 F2 N3 O3	7.59	418.1928	-3.3	-1.7	96	97	27	48	51	69	388	137, 145, 265
E21	Oxidative defluorination and monoOH	C22 H26 F N3 O3	8.04	400.2022	-2.8	-0.8	150	151	15	31	22	29	398	145, 177, 213, 233

Note: The peak areas in italics were retrieved by extension of the mass error values to 20 ppm as the amount of parent compound in these samples were saturating the detector.

Abbreviations: DiOH, dihydroxylation; GLUC, glucuronidation; MonoOH, monohydroxylation.

T A B L E 3 4’F-Cumyl]-5F-PICA metabolites with biotransformation, molecular formula, retention time, mass errors (minimum and maximum), exact mass (m/z) of protonated molecules and peak areas at 1-, 3- and 5-h incubation time

Met-ID	Compound name	Molecular formula	Retention time (min)	Obs m/z (M + H)	ppm min	ppm max	1 h #1 A/1000	1 h #2 A/1000	3 h #1 A/1000	3 h #2 A/1000	5 h #1 A/1000	5 h #2 A/1000	Grand total	Major fragment ions
M0	Parent	C23 H26 F2 N2 O	10.71	385.2085	-1.29	0.51	20 056	21 482	11 155	14 114	18 806	19 188	104 801	109, 118, 137, 144, 206, 232
M1	Oxidative defluorination	C23 H27 F N2 O2	8.65	383.2128	-1.8	0.1	460	583	164	261	1027	1129	3625	109, 118, 130, 137, 204, 230
M2	Oxidative defluorination, monoOH with dehydrogenation	C23 H25 F N2 O3	8.40	397.1917	-2.95	0.19	49	53	196	202	428	458	1385	109, 137, 156, 172, 200, 218
M3	N-dealkylation	C18 H17 F N2 O	7.96	297.1394	-2.53	-0.45	78	96	63	103	364	400	1105	118, 137, 144, 161
M4	Oxidative defluorination and monoOH	C23 H27 F N2 O3	6.93	399.2070	-3.63	-0.81	40	45	97	52	317	333	884	109, 137, 146, 160, 202, 220
M5	MonoOH	C23 H26 F2 N2 O2	8.74	401.2027	-3.05	-1.3	77	104	19	41	186	226	653	109, 134, 137, 148, 222, 248
M6	MonoOH + GLUC	C29 H34 F2 N2 O8	6.79	577.2347	-2.13	-1.28	14	17	62	61	114	117	387	137, 148, 222, 248, 265
M7	Oxidative defluorination, monoOH + GLUC	C29 H35 F N2 O9	5.50	575.2390	-2.18	-1.6	6	7	34	33	64	64	207	109, 137, 202, 220

(Continues)

TABLE 3 (Continued)

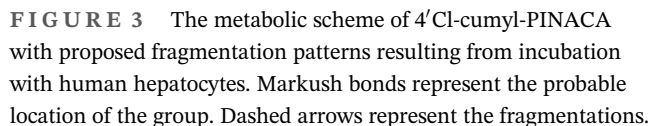
Met-ID	Compound name	Molecular formula	Retention time (min)	Obs m/z (M + H)	ppm min	ppm max	1 h #1 A/1000	1 h #2 A/1000	3 h #1 A/1000	3 h #2 A/1000	5 h #1 A/1000	5 h #2 A/1000	Grand total	Major fragment ions
M8	DiOH + GLUC	C ₂₉ H ₃₄ F ₂ N ₂ O ₉	6.95	593.2298	-1.65	-1.25	7	8	16	22	70	76	199	109, 137, 220, 238, 264, 281
M9	N-dealkylation and monoOH	C ₁₈ H ₁₇ FN ₂ O ₂	6.23	313.1341	-2.25	-1.77				3	80	88	171	109, 134, 137
M10	Oxidative defluorination, diOH and dehydrogenation	C ₂₃ H ₂₅ FN ₂ O ₄	6.81	413.1860	-2.7	-2.38	2	4	11	14	35	39	104	83, 137, 188, 216, 234, 260

Abbreviations: DiOH, dihydroxylation; GLUC, glucuronidation; MonoOH, monohydroxylation.

of 13.66 min (see Table 1). The most abundant metabolite was monohydroxylated (monoOH) with dehydrogenation at the pentyl tail chain (A1) followed by monoOH at the pentyl tail chain (A2). However, the metabolite abundance and area of 4'-Cl-cumyl-PINACA should be viewed with caution due to atypical increase of the parent area during 1- to 5-h incubation. Except for the trihydroxylated metabolite (triOH) (A11), where one hydroxylation was observed at the indazole ring, all other biotransformations were observed at the pentyl tail chain. These included dihydroxylations (diOH) (A3, A6), diOH with dehydrogenation (A5, A9), monoOH with glucuronidation (A8) and N-dealkylation metabolite (A10). Notably, no dechlorination at the head moiety was detected. Structures of the metabolites with respective fragmentation patterns are organized in a proposed metabolic pathway in Figure 3, and all MS and MS/MS spectra of the 4'-Cl-cumyl-PINACA metabolites are shown in the Supporting Information.

3.2 | The metabolic profile of 4'-F-cumyl-5F-PINACA

For 4'-F-cumyl-5F-PINACA, 21 metabolites (E1-E21) were identified which eluted between 5.71 and 9.70 min (see Table 2). The retention time of the parent compound was 11.43 min. Oxidative defluorination with and without additional monoOH were the two most abundant metabolites (E2 and E1, respectively), followed by monoOH on the fluoro-pentyl tail (E3 and E5) and N-dealkylation of the fluoro-pentyl tail (E4). Three of the metabolites detected were glucuronides (E6, E11 and E15) detected only in combinations with a second biotransformation. Of these, E6 glucuronide was complemented with oxidative defluorination while E11 and E15 were complemented with monoOH at the fluoro-pentyl tail. Oxidative defluorination was also observed for the head moiety leading to phenol formation (E14, E18 and E21). This biotransformation was accompanied by one monoOH at the head moiety (E21) or monoOH at the head moiety and fluoro-pentyl tail (E14 and E18). Other metabolites were monoOH with dehydrogenation (E7) in combination with oxidative defluorination (E12 and E13) and dihydrodiol formation (E10) in combination with monoOH at the fluoro-pentyl tail (E16 and E19), oxidative defluorination (E9) or diOH at the fluoro-pentyl tail (E20). All metabolite structures with the proposed fragmentation patterns are organized in a proposed metabolic pathway in Figure 4, and the MS and MS/MS spectra of all the metabolites are shown in the Supporting Information.



Ten metabolites were identified (M1–M10) for 4′F-cumyl-5F-PICA. These eluted between 5.50 and 8.74 min with the parent compound having the highest retention time of 10.70 min (see Table 3). The most abundant metabolites were oxidative defluorination (M1) and monoOH with dehydrogenation (M2), followed by N-dealkylation (M3).

For the second indazole compound, 4'F-cumyl-5F-PINACA, the three most common ion fragments were at m/z 233, 145 and 213. This is in agreement with the RESPONSE project, which reported their two most abundant fragments of m/z 233 and 145,²³ and Krotulski 2020,

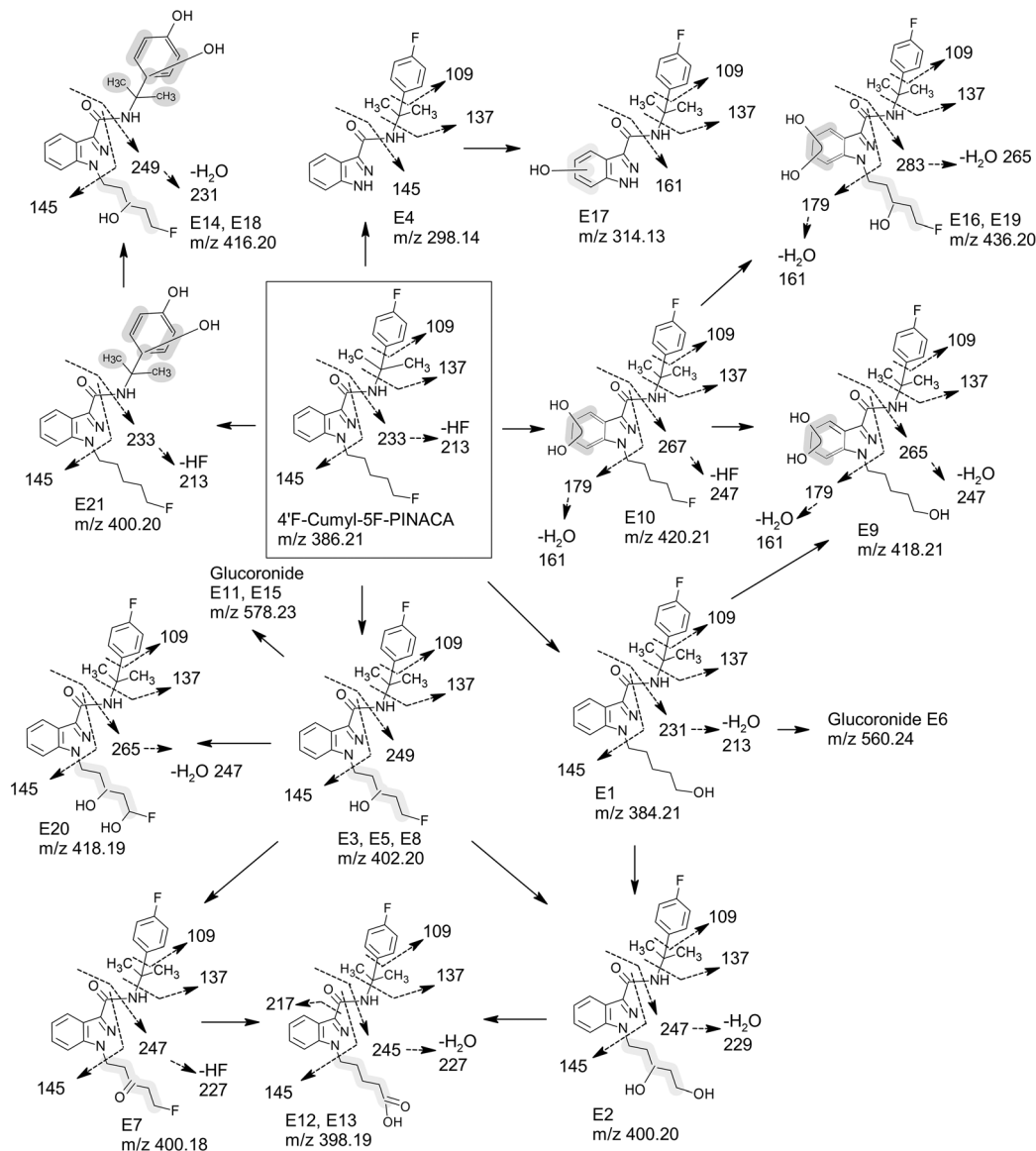


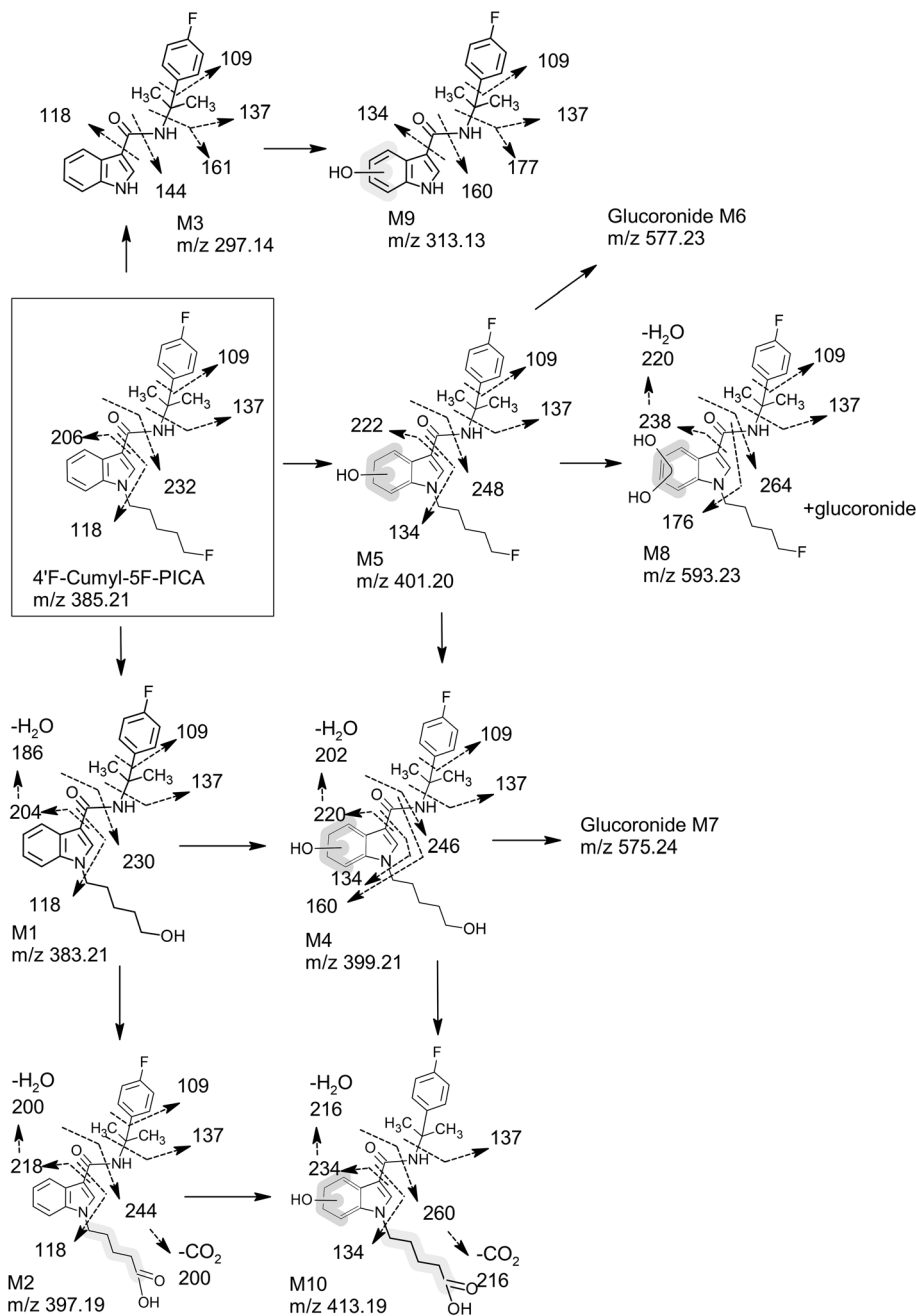
FIGURE 4 The metabolic scheme of 4'F-cumyl-5F-PINACA with proposed fragmentation patterns resulting from incubation with human hepatocytes. Markush bonds represent the probable location of the group. Dashed arrows represent the fragmentations.

who listed fragment ions of m/z 233, 137, 213, 250 and 177 in their LC-QToF-MS library.²⁵ The fragment of m/z 233 is related to the m/z 215 fragment of 4'Cl-cumyl-PINACA with an additional fluoro group at the terminal end of the pentyl tail. The fragment m/z 145 is the same as the fragment of 4'Cl-cumyl-PINACA with further N-dealkylation of the tail of fragment m/z 233. The fragment m/z 213 corresponds to a structure also related to the m/z 233 fragment with the cleavage of hydrogen fluoride. Interestingly, the m/z 213 fragment has also been observed by Staehli et al.²¹ and Bovens et al.²⁴ for 5F-cumyl-PINACA, but not for the 7-azaindole analogue, 5F-cumyl-P7AICA, which also has a fluoro-pentyl tail.^{21,24} Additionally, the fourth most abundant fragment

of 4'F-cumyl-5F-PINACA in this study was m/z 137, which corresponds to a fluoro-cumyl moiety.

For the indole compound, 4'F-cumyl-5F-PICA, the three most common fragment ions detected were m/z 206, 137 and 232, but m/z 144, which represents the indole core, was also present. These detected ions are different from those reported by the RESPONSE project, m/z 232 and 144.²³ In this study, the fragment ion m/z 144 was detected, although in smaller abundance, and ion m/z 248 from the RESPONSE project might be similar to the ion m/z 249 detected in this study. However, the differences between the LC-ESI and GC-EI have to be considered. The ion m/z 232 corresponds with a fluoro-pentylindole moiety with cleavage at the amide bond.

FIGURE 5 The metabolic scheme of 4'-F-cumyl-5F-PICA with proposed fragmentation patterns resulting from incubation with human hepatocytes. Markush bonds represent the probable location of the group. Dashed arrows represent the fragmentations.



moiety. For 4'Cl-cumyl-PINACA, nine out of 11 metabolites had biotransformations attached to the tail chain, as the fragment m/z 145 was consistent with the parent compound. These biotransformations were hydroxylations and dehydrogenations assigned by the presence of the fragment ions m/z 231 (an increase of 16 for hydrogen substitution with a hydroxyl group), m/z 247 (an increase of 32 for two hydrogen substitutions with two hydroxyl groups), 229 (an increase of 14 for two hydrogen substitutions with a carbonyl group) and m/z 245 (an increase of 30 for two hydrogen substitutions with a hydroxyl group and carbonyl group). Also, one glucuronide was detected for this compound, which was also associated with attachment to the tail as the fragment m/z 231 was observed. The tenth metabolite was N-dealkylation with characteristic m/z 145 fragment. The eleventh and final metabolite was triOH, where fragment m/z 161 indicated monoOH at the indazole moiety (an increase of 16 from the parent m/z 145 fragment) and m/z 263 indicated three hydroxylations in total at the indazole and tail moiety. Interestingly, triOH was not observed for the other two SCRA, 4'F-cumyl-5F-PINACA and 4'F-cumyl-5F-PICA.

One difference between 4'Cl-cumyl-PINACA, 4'F-cumyl-5F-PINACA and 4'F-cumyl-5F-PICA is the halogenated tail, which is common among novel SCRA. ^{1,5,9,21,28} For such SCRA, common biotransformation at the tail is oxidative dehalogenation to alcohol and further to carboxylic acid. ^{16,21,28} In this study, dehalogenation to alcohol was detected with the fragment of m/z 231 for 4'F-cumyl-5F-PINACA and m/z 230 for 4'F-cumyl-5F-PICA, which biotransformed from fragments 145 and 144, respectively, accounting for the -1 difference for indazole and indole moieties. Of both SCRA, oxidative defluorination at the tail was present in six out of 21 metabolites (46% of total metabolite abundance) for 4'F-cumyl-5F-PINACA and four out of 10 metabolites (70% of total metabolite abundance) for 4'F-cumyl-5F-PICA. The characterizing fragment ions for these were m/z 145 and 231 for 4'F-cumyl-5F-PINACA and m/z 118 and 230 for 4'F-cumyl-5F-PICA. Excluding N-dealkylation, 13 metabolites of 4'F-cumyl-5F-PINACA and three metabolites of 4'F-cumyl-5F-PICA preserved the terminal fluorine on the tail moiety. Additionally, non-oxidative dehalogenation at the tail or cumyl group was detected.

The oxidative defluorination at the cumyl moiety was only observed for 4'F-cumyl-5F-PINACA in combination with a hydroxylation at the cumyl moiety. For these metabolites (E14, E18 and E21), the usual m/z 137 fragment present in all other metabolite fragmentation patterns was absent. Instead, only the other characteristic fragments of m/z 145 and 233 (249 for the E14 and E18

with an additional hydroxyl group at the tail) were present in the mass spectra. It must be noted that biotransformations at fluorinated cumyl group are rarely detected due to the strong aromatic C (sp^2)-F bond and the reduced electron density in the aromatic ring lowering the rate of oxidation by P450. ¹⁰

All metabolite retention times and abundancies compared with each parent compound are shown in overlaid chromatograms in Figure 6. In the figure, due to contamination, only retention time is presented for E12 and E13 metabolites. The excluded chromatograms and the proposed structures of these metabolites can be found in the Supporting Information.

Overall, in this study, 4'F-cumyl-5F-PINACA had the largest number and widest variation in metabolites compared with the other two SCRA tested. In addition to the previously mentioned metabolites, it included two N-dealkylated metabolites, three glucuronides and four dihydrodiol metabolites.

4.3 | Trends in metabolic pattern

For the three SCRA tested, all of their metabolites were formed after 1-h incubation with the exception of the N-dealkylation with monoOH (M9) of 4'F-cumyl-5F-PICA, which was detected only in samples incubated for 3 and 5 h. MonoOH is a highly abundant and rapid biotransformation for all three parent compounds as the presence of monoOH with dehydrogenation is the most abundant metabolite for 4'Cl-cumyl-PINACA and monoOH area sharply decreases after 1-h incubation measurements for 4'F-cumyl-5F-PINACA and 4'F-cumyl-5F-PICA. For parent compounds with a fluorinated tail chain, the most abundant metabolites were oxidative defluorinations; however, these metabolites do not have a rapid area decrease after 1-h incubation and were still present in high abundance even after 5-h incubation. The N-dealkylation metabolites also had a high area value for compounds with a fluorinated tail chain; however, this biotransformation was not as common for 4'Cl-cumyl-PINACA. This could suggest that N-dealkylation is more common for compounds with a tail chain terminally altered with fluorine as observed by this study or a cyano group as observed by Staehli et al. ²¹

MonoOH and further hydroxylations on an indole moiety were more common (6/10 metabolites of 4'F-cumyl-5F-PICA) and more abundantly (28% of total metabolite peak area) observed than for its related indazole compound (5/21 metabolites of 4'F-cumyl-5F-PINACA and 5% of the total metabolite peak area). This trend should be viewed with caution as metabolite

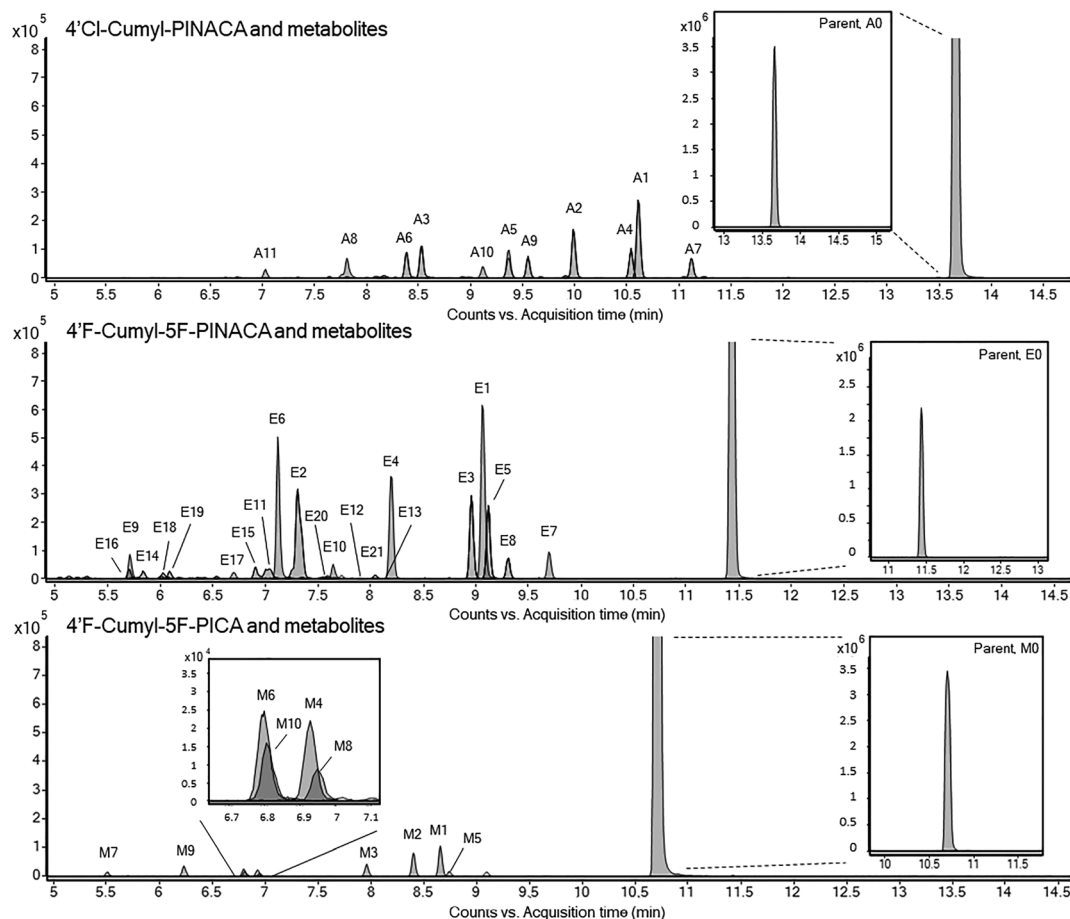


FIGURE 6 The overlaid chromatogram shows the abundance and the retention times of all the metabolites from 3-h incubation samples. 4'F-Cumyl-5F-PINACA peaks of E12 and E13 are excluded from this figure as their chromatogram showed contamination with higher abundance than the parent compound. The chromatograms of these metabolites are shown in the Supporting Information of 4'F-cumyl-5F-PINACA. For more observable peaks in 4'F-cumyl-5F-PICA chromatograms, metabolites M9 and M10 were taken from 5-h incubation samples. All the quantitative data of the peak areas are shown in Tables 1–3.

abundance compared with the parent compound was very different between both compounds; however, a similar trend was observed by Haschimi et al., where cumyl-CBMICA had slightly more detected biotransformations at the indole moiety (15/27 metabolites) than cumyl-CBMINACA at the indazole moiety (9/22 metabolites).²⁹ This is likely due to the shift in polarity as an additional nitrogen is introduced within the core ring structure. Even more, hydroxylation at the indazole ring for 4'Cl-cumyl-PINACA was detected in even smaller amounts than the other two SCRA, with only 1/11 metabolites with this biotransformation and 2% of the total metabolite peak areas.

Glucuronide metabolites were present in all three SCRA metabolic profiles, more commonly for the fluorinated compounds. The glycosidic bond formation was associated with the tail moieties, with the exception of the indole compound, 4'F-cumyl-5F-PICA. Based on the three detected glucuronides of the 4'F-cumyl-5F-PICA,

the bond is most likely formed at the hydroxylated indole group. This again shows the indole being more targeted as a biotransformation site than related indazole compounds.

The metabolism of 4'Cl-cumyl-PINACA, 4'F-cumyl-5F-PINACA and 4'F-cumyl-5F-PICA has shown to be similar to previously reported cumyl carboxamide SCRA, including cumyl-PINACA, 5F-cumyl-PINACA, cumyl-PICA and 5F-cumyl-PICA.^{16,20,21} The only outstanding and rare biotransformation metabolites were oxidative defluorination at the cumyl moiety, E21, and a further hydroxylation of tail, E14 and E18, of 4'F-cumyl-5F-PINACA.

Oxidative defluorination at aromatic structures has been previously detected for GW420867X, an antiviral HIV drug withdrawn from clinical trials³⁰; famitinib, currently in Phase III trials in cancer treatment^{31,32}; and sunitinib and gefitinib, both currently used in cancer treatment.^{33,34} From the listed pharmaceuticals, only

famitinib and sunitinib share the same fluorinated ring structure. Although these ring structures are not cumyl groups, the oxidative defluorination metabolites have created concerns about hepatotoxicity mostly due to downstream reactive quinoneimine formation^{31,33,35} and to a lesser extent formation of quinone imine in gefitinib metabolism.³⁴ This may give rise to a concern of additional hepatotoxicity from fluorinated aromatic NPS entering the market.

Furthermore, the presence and abundance of these metabolites can also be dependent on the interindividual genetical variability of the hepatic enzymes. In this study, a pool of 10 and 20 donor hepatocytes was used reflecting an average functional liver metabolism. Although the hepatocyte enzymatic activity (of 14 enzymes) is tested by the manufacturer, the genetic variability within the pool is unknown.

Furthermore, as these three SCRA have not been characterized before, it is uncertain if the proposed metabolic patterns and trends are universal; therefore, confirmational studies with the same or analogue compounds in the future are necessary to provide more certainty.

In this study, the parent compounds were still detectable with a large area value even after 5 h incubation with human hepatocytes. In comparison, cumyl-PINACA was detectable in human serum within 24 h after oral administration¹⁶ and cumyl-PICA and 5F-cumyl-PICA were still detectable after 24 h in rat plasma after intraperitoneal administration, which could also be true for the SCRA tested in this study. The rapid and similar metabolism of known related SCRA can make detection and distinction of compounds a complex task. However, metabolites of 4'Cl-cumyl-PINACA, 4'F-cumyl-5F-PINACA and 4'F-cumyl-5F-PICA are currently easily distinguishable due to their characteristically halogenated cumyl moieties and the formation of metabolites with additional hydroxyl groups with intact halogen groups at cumyl and/or terminal tail chain moieties.

5 | CONCLUSION

In human hepatocyte incubations, 11 metabolites of 4'Cl-cumyl-PINACA, 21 metabolites of 4'F-cumyl-5F-PINACA and 10 metabolites of 4'F-cumyl-5F-PICA were detected. These SCRA were found to undergo similar metabolism with common biotransformations, such as hydroxylation, oxidative defluorination, N-dealkylation and glucuronidations. Overall, hydroxylations were more common at the tail chain moieties; however, the core ring structure was more targeted for indole rather

than indazole compounds. Oxidative defluorination was the most abundant metabolite for both 4'F-cumyl-5F-PINACA and 4'F-cumyl-5F-PICA and, in combination with other biotransformations, was the most abundant biotransformation in each metabolic profile. N-dealkylation was more common for the compounds with a fluorinated tail chain moiety than the compound without (4'Cl-cumyl-PINACA). The metabolites with biotransformation at the cumyl moiety or dihydrodiol formation were only detected for 4'F-cumyl-5F-PINACA.

In summary, all three SCRA undergo a classical phase I metabolism in various combinations. Most of the metabolites include preserved halogen groups at the cumyl moiety, which, in combination with other metabolites, can be used as analytical biomarkers.

ACKNOWLEDGEMENTS

This project received funding from the Eurostars-2 Joint Programme (E! 113377, NPS-REFORM) with co-funding from the European Union's Horizon 2020 research and innovation programme, Sweden's Innovation Agency Vinnova (grant number 2019-03566) and the Strategic Research Area in Forensic Sciences (Strategiområdet for-ensiska vetenskaper, grant number 2016:7) at Linköping University.

CONFLICTS OF INTEREST

The authors declare that they have no conflict of interest.

ORCID

Darta Stalberga  <https://orcid.org/0000-0001-6712-652X>

Caitlyn Norman  <https://orcid.org/0000-0003-2322-0367>

REFERENCES

1. European Monitoring Centre for Drugs and Drug Addiction. *European Drug Report 2022: Trends and Developments*. Publications Office of the European Union, Luxembourg; 2022.
2. Pertwee RG, Howlett AC, Abood ME, et al. International union of basic and clinical pharmacology. LXXIX. Cannabinoid receptors and their ligands: beyond CB1 and CB2. *Pharmacol Rev*. 2010;62(4):588-631. doi:10.1124/pr.110.003004
3. Patel M, Finlay DB, Glass M. Biased agonism at the cannabinoid receptors—evidence from synthetic cannabinoid receptor agonists. *Cell Signal*. 2021;78:109865. doi:10.1016/j.cellsig.2020.109865
4. Huffman J, Padgett L. Recent developments in the medicinal chemistry of cannabimimetic indoles, pyrroles and indenenes. *Curr Med Chem*. 2005;12(12):1395-1411. doi:10.2174/0929867054020864
5. Banister SD, Stuart J, Kevin RC, et al. Effects of bioisosteric fluorine in synthetic cannabinoid designer drugs JWH-018, AM-2201, UR-144, XLR-11, PB-22, 5F-PB-22, apica, and STS-135. *ACS Chem Neurosci*. 2015;6(8):1445-1458. doi:10.1021/acschemneuro.5b00107

6. Doi T, Tagami T, Takeda A, Asada A, Sawabe Y. Evaluation of carboxamide-type synthetic cannabinoids as CB1/CB2 receptor agonists: difference between the enantiomers. *Forensic Toxicol.* 2017;36(1):51-60. doi:[10.1007/s11419-017-0378-5](https://doi.org/10.1007/s11419-017-0378-5)
7. Fattore L, Fratta W. Beyond THC: the new generation of cannabinoid designer drugs. *Front Behav Neurosci.* 2011;5:5. doi:[10.3389/fnbeh.2011.00060](https://doi.org/10.3389/fnbeh.2011.00060)
8. Tait RJ, Caldicott D, Mountain D, Hill SL, Lenton S. A systematic review of adverse events arising from the use of synthetic cannabinoids and their associated treatment. *Clin Toxicol.* 2015;54(1):1-13. doi:[10.3109/15563650.2015.1110590](https://doi.org/10.3109/15563650.2015.1110590)
9. Longworth M, Banister SD, Boyd R, et al. Pharmacology of CUMYL-carboxamide synthetic cannabinoid new psychoactive substances (NPS) CUMYL-Bica, Cumyl-pica, Cumyl-5F-PICA, CUMYL-5F-PINACA, and their analogues. *ACS Chem Neurosci.* 2017;8(10):2159-2167. doi:[10.1021/acscchemneuro.7b00267](https://doi.org/10.1021/acscchemneuro.7b00267)
10. Johnson BM, Shu Y-Z, Zhuo X, Meanwell NA. Metabolic and pharmaceutical aspects of fluorinated compounds. *J Med Chem.* 2020;63(12):6315-6386. doi:[10.1021/acs.jmedchem.9b01877](https://doi.org/10.1021/acs.jmedchem.9b01877)
11. Gamage TF, Farquhar CE, Lefever TW, et al. Molecular and behavioral pharmacological characterization of abused synthetic cannabinoids MMB- and MDMB-FUBINACA, MN-18, NNEI, Cumyl-pica, and 5-fluoro-cumyl-pica. *J Pharmacol Exp Ther.* 2018;365(2):437-446. doi:[10.1124/jpet.117.246983](https://doi.org/10.1124/jpet.117.246983)
12. Asada A, Doi T, Tagami T, et al. Cannabimimetic activities of CUMYL carboxamide-type synthetic cannabinoids. *Forensic Toxicol.* 2017;36(1):170-177. doi:[10.1007/s11419-017-0374-9](https://doi.org/10.1007/s11419-017-0374-9)
13. Bowden MJ, Williamson JPB. *Cannabinoid compounds.* 2014.
14. Zangani C, Schifano F, Napoletano F, et al. The e-psychonauts' 'spiced' world; assessment of the synthetic Cannabinoids' information available online. *Curr Neuropsychopharmacol.* 2020;18(10):966-1051. doi:[10.2174/1570159x18666200302125146](https://doi.org/10.2174/1570159x18666200302125146)
15. NPS and Related Compounds Database. 2015. https://www.policijsi/apps/nfl_response_web/seznam.php. Accessed November 4, 2022.
16. Angerer V, Franz F, Moosmann B, Bisel P, Auwärter V. 5F-cumyl-PINACA in 'e-liquids' for electronic cigarettes: comprehensive characterization of a new type of synthetic cannabinoid in a trendy product including investigations on the in vitro and in vivo phase I metabolism of 5F-cumyl-PINACA and its non-fluorinated analog cumyl-PINACA. *Forensic Toxicol.* 2018;37(1):186-196. doi:[10.1007/s11419-018-0451-8](https://doi.org/10.1007/s11419-018-0451-8)
17. Diao X, Huestis MA. Approaches, challenges, and advances in metabolism of new synthetic cannabinoids and identification of optimal urinary marker metabolites. *Clin Pharmacol Ther.* 2016;101(2):239-253. doi:[10.1002/cpt.534](https://doi.org/10.1002/cpt.534)
18. Tai S, Fantegrossi WE. Synthetic cannabinoids: pharmacology, behavioral effects, and abuse potential. *Curr Addict Rep.* 2014;1(2):129-136. doi:[10.1007/s40429-014-0014-y](https://doi.org/10.1007/s40429-014-0014-y)
19. Zaitso K, Nakayama H, Yamanaka M, et al. High-resolution mass spectrometric determination of the synthetic cannabinoids Mam-2201, AM-2201, AM-2232, and their metabolites in postmortem plasma and urine by LC/Q-TOFMS. *Int J Leg Med.* 2015;129(6):1233-1245. doi:[10.1007/s00414-015-1257-4](https://doi.org/10.1007/s00414-015-1257-4)
20. Kevin RC, Lefever TW, Snyder RW, et al. In vitro and in vivo pharmacokinetics and metabolism of synthetic cannabinoids cumyl-pica and 5F-cumyl-pica. *Forensic Toxicol.* 2017;35(2):333-347. doi:[10.1007/s11419-017-0361-1](https://doi.org/10.1007/s11419-017-0361-1)
21. Staeheli SN, Poetzsch M, Veloso VP, et al. In vitro metabolism of the synthetic cannabinoids cumyl-PINACA, 5F-cumyl-PINACA, cumyl-4CN-BINACA, 5F-cumyl-p7aica and cumyl-4cn-B7AICA. *Drug Test Anal.* 2017;10(1):148-157. doi:[10.1002/dta.2298](https://doi.org/10.1002/dta.2298)
22. Tveden-Nyborg P, Bergmann TK, Jessen N, Simonsen U, Lykkesfeldt J. BCPT policy for experimental and clinical studies. *Basic Clin Pharmacol Toxicol.* 2020;128(1):4-8. doi:[10.1111/bcpt.13492](https://doi.org/10.1111/bcpt.13492)
23. National Forensic Laboratory of Slovenia. Analytical Report. 4Cl-CUMYL-5F-PINACA (C22H26CIN3O). Ljubljana; 2018.
24. Bovens M, Bissig C, Staeheli SN, Poetzsch M, Pfeiffer B, Kraemer T. Structural characterization of the new synthetic cannabinoids Cumyl-PINACA, 5F-cumyl-PINACA, cumyl-4CN-BINACA, 5F-cumyl-p7aica and cumyl-4cn-B7AICA. *Forensic Sci Int.* 2017;281:98-105. doi:[10.1016/j.forsciint.2017.10.020](https://doi.org/10.1016/j.forsciint.2017.10.020)
25. Krotulski AJ, Varnum SA, Wengryniuk SE, Valentine AM, Logan BK. *A More Timely Process for Identifying and Analyzing Trends of Emerging Novel Psychoactive Substances in the United States.* Vol. 335; 2019.
26. Banister SD, Adams A, Kevin RC, et al. Synthesis and pharmacology of new psychoactive substance 5F-CUMYL-p7aica, a scaffold-hopping analog of synthetic cannabinoid receptor agonists 5F-CUMYL-PICA and 5F-CUMYL-PINACA. *Drug Test Anal.* 2018;11(2):279-291. doi:[10.1002/dta.2491](https://doi.org/10.1002/dta.2491)
27. Kleis J, Germerott T, Halter S, et al. The synthetic cannabinoid 5F-MDMB-PICA: a case series. *Forensic Sci Int.* 2020;314:110410. doi:[10.1016/j.forsciint.2020.110410](https://doi.org/10.1016/j.forsciint.2020.110410)
28. Mogler L, Franz F, Rentsch D, et al. Detection of the recently emerged synthetic cannabinoid 5F-MDMB-PICA in 'legal high' products and human urine samples. *Drug Test Anal.* 2017;10(1):196-205. doi:[10.1002/dta.2201](https://doi.org/10.1002/dta.2201)
29. Haschimi B, Grafinger KE, Pulver B, et al. New synthetic cannabinoids carrying a cyclobutyl methyl side chain: human phase I metabolism and data on human cannabinoid receptor 1 binding and activation of cumyl-CBMICA and cumyl-cbminaca. *Drug Test Anal.* 2021;13(8):1499-1515. doi:[10.1002/dta.3038](https://doi.org/10.1002/dta.3038)
30. Mutch PJ, Dear GJ, Ismail IM. Formation of a defluorinated metabolite of a quinoxaline antiviral drug catalysed by human cytochrome P450 1A2. *J Pharm Pharmacol.* 2001;53(3):403-408. doi:[10.1211/0022357011775479](https://doi.org/10.1211/0022357011775479)
31. Xie C, Zhou J, Guo Z, et al. Metabolism and bioactivation of famitinib, a novel inhibitor of receptor tyrosine kinase, in cancer patients. *Br J Pharmacol.* 2013;168(7):1687-1706. doi:[10.1111/bph.12047](https://doi.org/10.1111/bph.12047)
32. List of Clinical Trials Involving Famitinib. Home - ClinicalTrials.gov. <https://clinicaltrials.gov/ct2/results?cond=famitinib&term=&cntry=&state=&city=&dist=>. Accessed November 2, 2022.
33. Burnham EA, Abouda AA, Bissada JE, et al. Interindividual variability in cytochrome P450 3A and 1A activity influences sunitinib metabolism and bioactivation. *Chem Res Toxicol.* 2022;35(5):792-806. doi:[10.1021/acs.chemrestox.1c00426](https://doi.org/10.1021/acs.chemrestox.1c00426)
34. Li X, Kamenecka TM, Cameron MD. Bioactivation of the epidermal growth factor receptor inhibitor gefitinib: implications

for pulmonary and hepatic toxicities. *Chem Res Toxicol.* 2009; 22(10):1736-1742. doi:[10.1021/tx900256y](https://doi.org/10.1021/tx900256y)

35. Amaya GM, Durandis R, Bourgeois DS, et al. Cytochromes P450 1A2 and 3A4 catalyze the metabolic activation of Sunitinib. *Chem Res Toxicol.* 2018;31(7):570-584. doi:[10.1021/acs.chemrestox.8b00005](https://doi.org/10.1021/acs.chemrestox.8b00005)

SUPPORTING INFORMATION

Additional supporting information can be found online in the Supporting Information section at the end of this article.

How to cite this article: Stalberga D, Ingvarsson S, Bessa G, et al. Metabolism studies of 4'-Cl-CUMYL-PINACA, 4'-F-CUMYL-5F-PINACA and 4'-F-CUMYL-5F-PICA using human hepatocytes and LC-QTOF-MS analysis. *Basic Clin Pharmacol Toxicol.* 2023;132(3):263-280. doi:[10.1111/bcpt.13829](https://doi.org/10.1111/bcpt.13829)